GASTROINTESTINAL AND LIVER PHYSIOLOGY

Am J Physiol Gastrointest Liver Physiol 322: G21–G33, 2022. First published November 3, 2021; doi:10.1152/ajpgi.00266.2021

RESEARCH ARTICLE

Translational Physiology

Activation of autophagy during normothermic machine perfusion of discarded livers is associated with improved hepatocellular function

Anders Ohman,^{1*} [©] Siavash Raigani,^{2,3*} John C. Santiago,¹ Megan G. Heaney,¹ Joan M. Boylan,¹ Nicola Parry,⁴ Cailah Carroll,² Sofia G. Baptista,² Korkut Uygun,³ Philip A. Gruppuso,¹ Jennifer A. Sanders,^{1*} and Heidi Yeh^{2*}

¹Department of Pediatrics, Rhode Island Hospital and Brown University, Providence, Rhode Island; ²Division of Transplant Surgery, Massachusetts General Hospital, Boston, Massachusetts; ³Center for Engineering in Medicine and Surgery, Massachusetts General Hospital and Harvard Medical School, Boston, Massachusetts; and ⁴Section of Pathology, Cummings School of Veterinary Medicine at Tufts University, North Grafton, Massachusetts

Abstract

Liver transplantation is hampered by a severe shortage of donor organs. Normothermic machine perfusion (NMP) of donor livers allows dynamic preservation in addition to viability assessment before transplantation. Little is known about the injury and repair mechanisms induced during NMP. To investigate these mechanisms, we examined gene and protein expression changes in a cohort of discarded human livers, stratified by hepatocellular function, during NMP. Six human livers acquired through donation after circulatory death (DCD) underwent 12 h of NMP. Of the six livers, three met predefined criteria for adequate hepatocellular function. We applied transcriptomic profiling and protein analysis to evaluate temporal changes in gene expression during NMP between functional and nonfunctional livers. Principal component analysis segregated the two groups and distinguished the various perfusion time points. Transcriptomic analysis of biopsies from functional livers indicated robust activation of innate immunity after 3 h of NMP followed by enrichment of prorepair and prosurvival mechanisms. Nonfunctional livers demonstrated delayed and persistent enrichment of markers of innate immunity. Functional livers demonstrated effective induction of autophagy, a cellular repair and homeostasis pathway, in contrast to nonfunctional livers. In conclusion, NMP of discarded DCD human livers results in innate immune-mediated injury, while also activating autophagy, a presumed mechanism for support of cellular repair. More pronounced activation of autophagy was seen in livers that demonstrated adequate hepatocellular function.

NEW & NOTEWORTHY We demonstrate that ischemia-reperfusion injury occurs in all livers during NMP, though there are notable differences in gene expression between functional and nonfunctional livers. We further demonstrate that activation of the liver's repair and homeostasis mechanisms through autophagy plays a vital role in the graft's response to injury and may impact liver function. These findings indicate that liver autophagy might be a key therapeutic target for rehabilitating the function of severely injured or untransplantable livers.

autophagy; ischemia reperfusion injury; liver transplantation; machine perfusion; normothermic

INTRODUCTION

http://www.ajpgi.org

Liver transplantation (LT) remains the only effective treatment for end-stage liver disease. Despite major progress in the safety and efficacy of LT, access to this life-saving procedure is limited because of a substantial organ shortage that results in significant waitlist mortality. Further compounding the shortage is the high discard rate of procured organs stemming from the increased risk of graft loss and dysfunction in livers transplanted from extended-criteria donors (1). Livers from donation after circulatory death (DCD) face

increased scrutiny due to the additional warm ischemic time, resulting in up to 30% of recovered DCD grafts being turned down for transplant in the United States (2).

Machine perfusion technology has emerged in the past decade as an effective method of improving graft preservation and decreasing discard rates (3–5). Normothermic machine perfusion (NMP) allows real-time evaluation of liver function and viability assessment, providing additional objective data to the transplant surgeon before committing a recipient to LT. However, it is not clear whether NMP actually improves graft quality over immediate implantation or is just a superior



^{*} A. Ohman and S. Raigani contributed equally to this work. J. A. Sanders and H. Yeh contributed equally to this work. Correspondence: H. Yeh (hyeh@mgh.harvard.edu); J. A. Sanders (jennifer_sanders@brown.edu). Submitted 17 August 2021 / Revised 11 October 2021 / Accepted 17 October 2021

preservation modality that happens to provide functional metrics. Recent work by Jassem et al. (6) compared transcriptional changes in the immediate postimplantation period of LT among donation after brain death (DBD) livers preserved by NMP versus static cold storage. Livers preserved with NMP demonstrated more robust enrichment of repair and regenerative pathways after reperfusion in situ. However, there was no examination of pathway activation during preservation (7). Furthermore, all the livers studied were determined to be functional and transplantable after preservation. Thus, these studies could not determine whether the postreperfusion changes that were observed represented functionally significant changes in the status of the donor tissue.

Despite growing adoption of NMP in the clinical setting, knowledge of the physiological changes that occur during ex situ perfusion is still limited. In the present study, we aimed to investigate the early-phase injury and repair mechanisms that might occur during normothermic machine perfusion of discarded DCD human livers, comparing grafts with and without adequate hepatocellular function, thereby providing a functional context for our work. Understanding the mechanistic differences between the patterns of injury and repair in these grafts will help in developing potential therapeutics for rehabilitation of currently discarded livers (3, 8), thereby increasing the pool of transplantable organs.

MATERIALS AND METHODS

Donor Livers

Six human donor livers with similar donor demographics were chosen for further analysis from a previously reported research cohort of machine-perfused discarded human livers (8). All six livers were DCD livers without significant steatosis and were rejected for transplant by all transplant centers in the respective donor service area. Reasons for discard included a combination of DCD status, donor age, and length of warm ischemic time. Human livers were procured in standard fashion through two organ

procurement organizations (OPOs): New England Donor Services (Waltham, MA) and LiveOnNewYork (New York, NY). Informed consent was obtained from donors by the OPOs. Table 1 describes the donor demographics for each organ. The Massachusetts General Hospital and Lifespan Institutional Review Boards, as well as the two OPOs, approved this study (No. 2011P001496). No organs were procured from prisoners and no vulnerable populations were included in this study.

Procurement of Grafts

Procurement techniques based on donation after circulatory death followed standard methods. Donor livers were flushed in situ with University of Wisconsin solution. Total warm ischemic time (WIT) was defined as the period from extubation to cold flush. Functional WIT was defined as the period from asystole to cold flush. Cold ischemic time was defined from cold flush to initiation of machine perfusion. After transport to the laboratory under static cold storage, livers underwent standard back bench preparation for machine perfusion (Fig. 1A) (9).

Machine Perfusion

Grafts were perfused on the Liver Assist device (Organ Assist, Groningen, Netherlands) using a previously described protocol (8). Briefly, perfusate composition consisted of O + packed red blood cells, human albumin, lactated Ringer solution, and heparin. Bile salts (taurocholate) and lipid-free parenteral nutrition were continuously infused. Perfusate, bile, and tissue biopsies were collected and analyzed at multiple time points (Fig. 1B). Grafts were deemed to demonstrate adequate hepatocellular function if they satisfied the criteria reported by Mergental et al. (3), namely, perfusate lactate < 2.5 mmol/L and two or more of the following minor criteria within 4 h of starting perfusion: 1) perfusate pH \geq 7.30 without supplemental bicarbonate, 2) arterial flow \geq 150 mL/min and portal flow \geq 500 mL/ min, 3) evidence of glucose metabolism, 4) bile production, and 5) visually assessed homogenous perfusion.

Table 1. Detailed characteristics of discarded grafts undergoing normothermic machine perfusion

	Adequate Hepatocellular Function (n = 3 subjects)			Inadequate Hepatocellular Function ($n = 3$ subjects)			P Value
Liver no.	F1	F2	F3	N1	N2	N3	
Total WIT, min	28	24	33	23	26	70	0.83
Functional WIT, min	8	8	12	11	9	11	0.50
CIT, h	11.6	5	7.6	6	13.1	6.1	0.83
Donor age, yr	60	58	59	55	21	56	0.0495
Sex	F	M	M	F	M	F	0.50
BMI, kg/m ²	24.5	28.3	27.3	24.6	27.4	44	0.51
Macrosteatosis, %	0	5	2	0	0	0	0.12
Microsteatosis, %	10	0	0	0	0	0	0.32
AST, U/L	39	41	57	24	82	138	0.51
ALT, U/L	27	22	38	11	97	161	0.51
Total bilirubin, mg/dL	0.6	0.9	0.4	0.2	0.4	0.4	0.10
ALP, U/L	95	36	31	94	234	494	0.13

Macrosteatosis defined as large droplet steatosis with nuclear displacement, provided as % of entire tissue field evaluated. Microsteatosis defined as small droplet steatosis without nuclear displacement, provided as % of entire tissue field evaluated. Aspartate aminotransferase (AST), alanine aminotransferase (ALT), total bilirubin, and alkaline phosphatase (ALP) levels indicate last available values before procurement. Group comparisons made using the Wilcoxon rank-sum (Mann-Whitney U) or Fisher's exact test, where appropriate. BMI, body mass index (kg/m²); CIT, cold ischemic time in minutes; F, female; M, male; WIT, warm ischemic time in minutes. Boldface value is a significant P value.

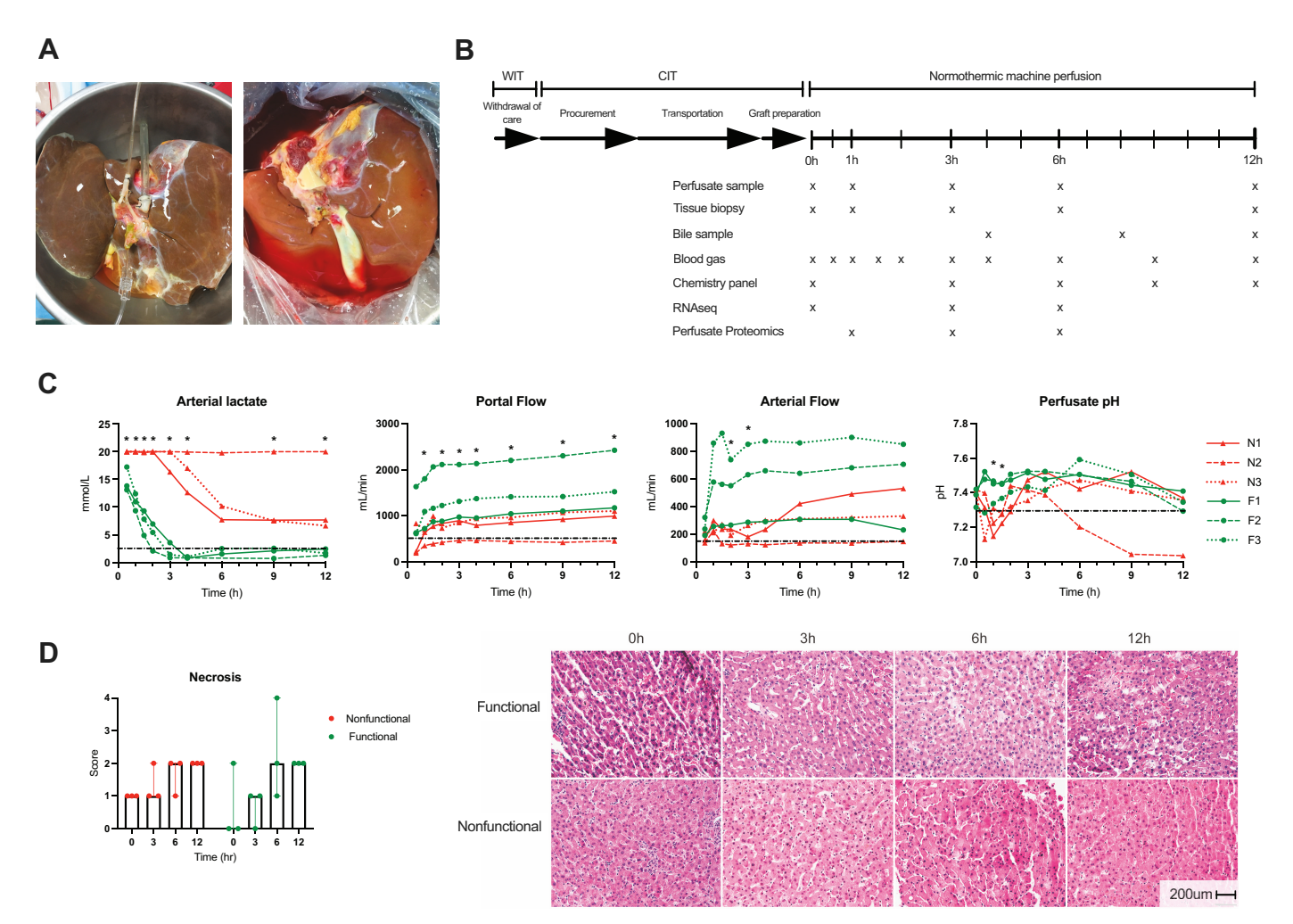


Figure 1. Study schematic and perfusion metrics. A: representative images of two human livers being prepared for machine perfusion. B: study schematic indicating periods of warm and cold ischemia during procurement followed by normothermic machine perfusion. Data and sample collection time points are indicated by "x" under the perfusion time bar. C: criteria used to determine hepatocellular function are shown for individual livers (red: nonfunctional, green: functional livers are primarily characterized by the ability to clear lactate below the 2.5 mmol/L threshold. Dotted black line indicates criteria thresholds. *P < 0.05 for group comparison at indicated time point. Lactate assay upper limit is 20 mmol/L. D: hepatocellular necrosis scores at individual time points demonstrate no significant difference between groups. Representative H&E images of functional and nonfunctional livers are shown. Scale bar: 200 microns. CIT, cold ischemic time; H&E, hematoxylin and eosin; F, functional liver; N, nonfunctional liver; WIT, warm ischemic time.

Cholangiocellular (biliary) functional metrics according to van Leeuwen (10) were measured but not used for functional stratification due to technical issues with bile collection in two livers.

Perfusate Analysis and Plasma Proteomics

Perfusate collected at the indicated time points was centrifuged at 5,000 g and the plasma collected and stored at -80°C for later analysis. Enzyme-linked immunosorbent assays (ELISAs) were performed for various proteins according to manufacturers' guidelines (Supplemental S1 Methods; all Supplemental Methods and Figs. are available at https://doi.org/10.5281/zenodo.5206547).

Proteomic profiling of trypsinized perfusate proteins was performed following albumin depletion in collaboration with the University of Arkansas Medical Sciences Proteomics Core. The equipment used, protein processing, and analysis are detailed in the Supplemental S2 Methods.

Total RNA Purification, Sequencing, and Analysis

Core needle biopsies taken immediately before perfusion and after 3 and 6 h of perfusion were used for transcriptome sequencing on an Illumina HiSeq 4000 using nine PCR cycles by GENEWIZ (South Plainfield, NJ). Tissue collection, purification, and bioinformatic analysis are detailed in the Supplemental S3 Methods. The differential gene expression threshold for significance was set to a Benjamini–Hochberg false discovery rate (FDR) of <0.05. Raw sequence data have been deposited in the Gene Expression Omnibus with Accession No. GSE165568.

Histology and Immunohistochemistry

Core needle biopsies taken from the right liver lobe at indicated intervals were fixed in formalin and embedded in paraffin. Hematoxylin and eosin (H&E) staining was performed on all biopsies to assess the degree of necrosis and



inflammatory cell infiltrate. A pathologist evaluated and scored all slides in a blinded manner using a semiquantitative scoring scheme (Supplemental S4 Methods). Immunohistochemistry methods and antibodies used are available in the Supplemental S5 Methods.

Western Blots

Sequential wedge biopsies from the right lobe of each liver were performed at indicated intervals, flash frozen in liquid nitrogen, and stored at -80° C. Tissue samples (20 mg) were homogenized and Western immunoblots performed as previously described (11). A full list of antibodies used is provided in the Supplemental S6 Methods.

Statistical Analysis

Categorical data are presented as median with interquartile range (IQR) and frequency data as percentages. For statistical tests not related to RNA sequencing or proteomic analysis, the Wilcoxon rank-sum test (Mann-Whitney U) and Fisher's exact test were used for group comparisons. A two-way analysis of variance (ANOVA) was used for comparisons between groups with repeated measures over time. The threshold for statistical significance was set at <0.05. Analyses were conducted using GraphPad Prism 8 (San Diego, CA) and Stata 15 (College Station, TX).

RESULTS

Assessment of Hepatocellular Function during **Normothermic Perfusion**

Donor demographics for the six study livers are provided in Table 1. Machine perfusion criteria used to determine whether each liver demonstrated adequate (functional) or inadequate (nonfunctional) hepatocellular function are shown in Fig. 1C and Supplemental Fig. S1. Functional livers (F1-F3) demonstrated evidence of increased glucose metabolism and increased urea synthesis over time (Supplemental Fig. S1). Although some nonfunctional livers (N1-N3) were able to meet minor criteria, all failed to meet the perfusate lactate threshold. Aspartate aminotransferase (AST) and alanine aminotransferase (ALT) levels (Supplemental Fig. S1) were higher for the functional livers than for the nonfunctional livers at 1 and 3 h of perfusion, though levels plateaued thereafter. In comparison, nonfunctional livers demonstrated AST and ALT levels that increased but were, in general, lower than the levels seen with the functional livers. Bile volume and cholangiocellular functional metrics are presented in Supplemental Fig. S2, though statistical comparisons were limited by technical errors with bile collection in two functional livers. H&E staining demonstrated an increase in percent necrosis after initiation of NMP in both groups, with all livers demonstrating up to 30% histologic necrosis by 12 h of perfusion (Fig. 1D).

Principal Component Analysis of the Transcriptomic Analyses Discriminates Functional from Nonfunctional Livers

Principal component analysis (PCA) demonstrated distinct changes in gene expression at 0 h (preperfusion), 3 h,

and 6 h of NMP among individual livers. The preperfusion gene expression profiles clustered together by hepatocellular function then diverged further once perfusion was initiated. Functional livers continued to cluster together after 3 and 6 h of NMP, whereas the nonfunctional livers demonstrated dissimilar profiles with respect to one another (Fig. 2A). Principal component 1 (PC1), which accounted for 28.3% of the variation in differentially expressed genes (DEG), captured the time-dependent changes in gene expression. The functional livers demonstrated a consistent transcriptional shift at each 3-h interval compared with lower magnitude changes in the nonfunctional livers. Analysis of the top 10% of genes contributing to PC1 revealed enrichment of gene ontology (GO) terms related to gene transcription and protein synthesis. Detailed examination of the temporal response of these genes revealed a marked increase in expression by 6 h of perfusion in the functional compared with nonfunctional livers (Fig. 2B).

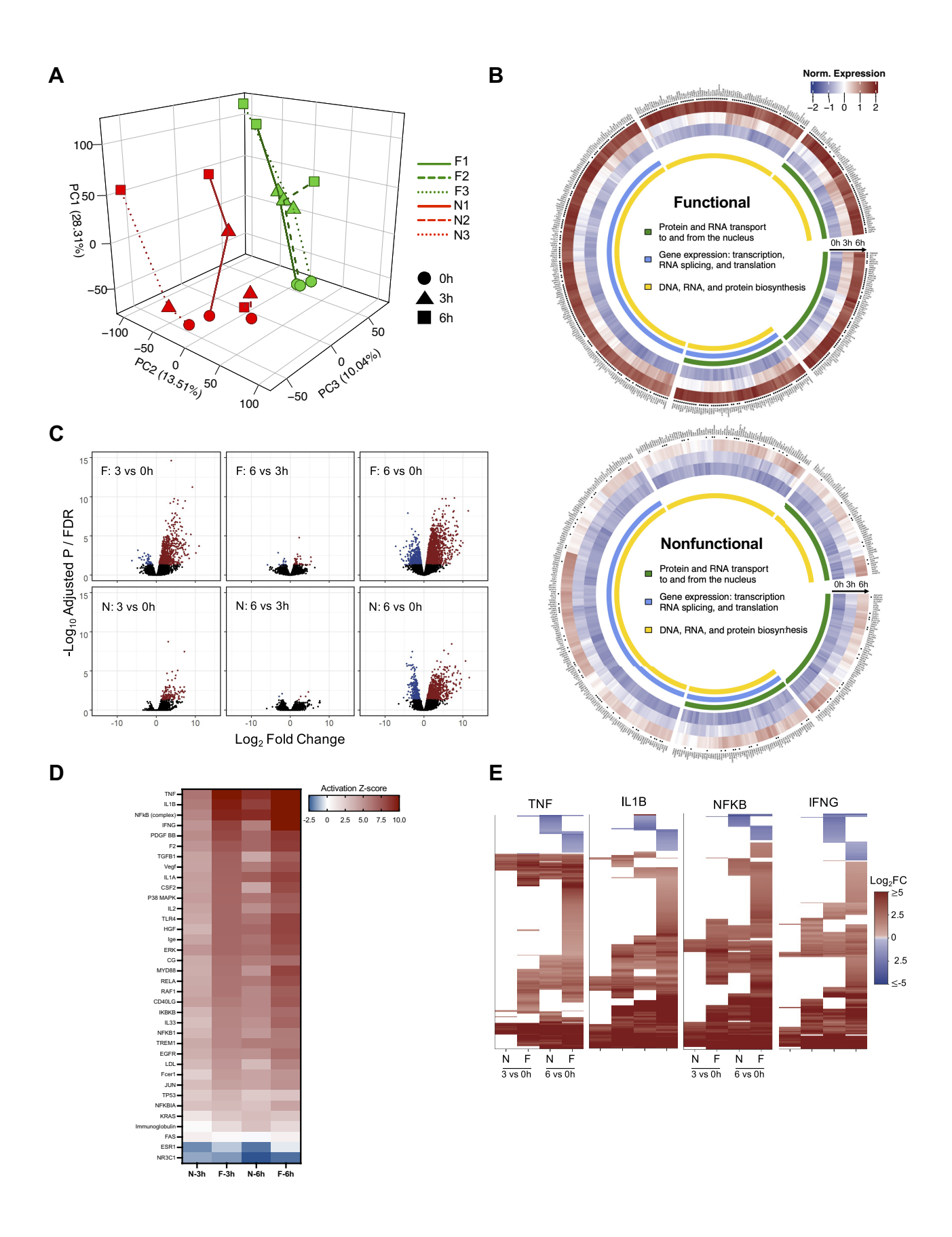
Principal component 2 did not distinguish any notable cellular processes despite accounting for 13.5% of the variation in DEG. Conversely, principal component 3 (PC3), representing 10.0% of the variation, was able to effectively discriminate functional from nonfunctional livers. The top 10% of genes contributing to PC3 were involved in GO cellular components related to extracellular vesicles and exosomes, endoplasmic reticulum, and membrane components, though none of the individual genes met the FDR cutoff for significance (Supplemental Fig. S3).

Transcription shifts captured by principal components were remarkably reflective of each liver's hepatocellular functional profile. For example, the nominal transcriptional shift in nonfunctional livers after initiation of NMP appeared to correspond with a delay in lactate clearance and perfusate pH stability in the first several hours of NMP. Furthermore, liver N2 demonstrated minimal changes in principal components compared with other livers, consistent with that liver's poor functional profile (lowest vascular flows, no evidence of lactate clearance, persistent metabolic acidosis, rising AST/ ALT). Interestingly, liver N1 demonstrated changes over time most similar to the functional livers based on PC1 and PC2 but diverged with the addition of PC3 (Supplemental Fig. S4).

Overview of Differential Gene Expression

Although individual livers clustered according to function with PCA, this was less apparent with comparison of timestatic gene sets between groups. Of the \sim 14,000 transcripts sequenced, only two genes (ARL16, NLGN2) were significantly different (FDR < 0.05) between functional and nonfunctional livers at the preperfusion time point. No genes were significant at 3 h. In contrast, 53 genes were differentially expressed at 6 h of perfusion (Supplemental Data Set S1; all Supplemental Data Sets are available at https://doi. org/10.5061/dryad.f7m0cfxx0). However, Ingenuity Pathway Analysis (IPA) did not reveal significant enrichment of any canonical pathways (CPs) or upstream regulators (URs) related to this gene set.

Analyses based on the temporal changes in gene expression during NMP relative to the preperfusion baseline were more informative of the physiological differences between



functional and nonfunctional livers during perfusion. Volcano plots showed that functional livers responded to NMP at 3 h with a robust and statistically significant upregulation of genes (Fig. 2C). This was followed by both upregulation and downregulation of numerous genes at 6 h. In contrast, nonfunctional livers upregulated expression of only a handful of genes at 3 h. This was followed with a greater degree of change in gene expression (both upregulation and downregulation) at 6 h.

Using IPA, we identified canonical pathways and URs associated with the temporal differential gene expression unique to the two experimental groups. In functional livers, over 25 pathways related to inflammation and innate immunity were enriched at 3 h, whereas nonfunctional livers only had four significant pathways and many fewer genes in each pathway (Supplemental Fig. S5). By 6 h, there was a shift in significant pathways to those associated with survival, protein ubiquitination, and growth in functional livers. The significant pathways in the nonfunctional livers were similar to those seen in the functional livers at 3 h of perfusion. The URs displayed similar temporal shifts (Supplemental Fig. S5). Activation Z-scores of significant URs related to innate immunity were higher in functional compared with nonfunctional livers after 3 h of NMP, indicating more marked induction of downstream gene targets in the early perfusion phase in the functional livers. By 6 h of NMP, active URs in the nonfunctional livers more closely resembled those of the functional livers (Fig. 2D). Despite this, when the top four URs were examined for downstream signaling, the two groups differed greatly in activation of their gene targets (Fig. 2E). Results using CiiiDER (12) to identify enriched transcription factor binding sites in the promoter regions of the differentially expressed genes were very similar to those obtained using IPA (Supplemental Data Set S2).

Ischemia-Reperfusion Injury and Innate Immune **Activation**

As noted earlier, the changes in gene expression that occurred during NMP suggested activation of innate immunity based on canonical pathways identified using pathway analysis (Fig. 3A). Functional livers demonstrated early enrichment of Toll-like receptor, high mobility group box 1, and interleukin-6 (IL-6) signaling pathways, among several others. Nonfunctional livers demonstrated activation of only the IL-6 canonical pathway after 3 h of NMP. However, after 6 h of perfusion, the nonfunctional livers displayed an expression profile that resembled that of the functional group at 3 h, whereas the functional group revealed pathway activation indicative of cell turnover and survival. These findings indicated that nonfunctional livers during NMP are distinguished by delayed onset of innate immune signaling. Examination of H&E stained liver biopsies supported these findings, with significantly more lobular and portal inflammatory cell infiltrates seen in nonfunctional livers (Fig. 3, B and C).

Given the findings related to immune activation, we analyzed damage-associated molecular patterns (DAMPs; Fig. 3D) and cytokines (Fig. 3E) in the circulating perfusate. Results were similar between groups at multiple time points when analyzed by ELISA. This was unexpected given the divergent expression profiles of the downstream gene targets noted earlier (Fig. 2E). To determine the presence of proteins differentiating functional from nonfunctional livers, we also performed untargeted plasma proteomics to further assess the DAMP and cytokine response to NMP. This revealed numerous enriched proteins varying between groups after 1, 3, and 6 h of perfusion, though only eight proteins remained statistically significant when a stringent FDR cutoff of <0.05 was applied (all at 3 h of NMP; Supplemental Fig. S6). Within this subset, none was directly related to DAMP or cytokine signaling (Supplemental Data

Role of the Unfolded Protein Response and Autophagy in Hepatocellular Function

Given the notable injury profile differences between functional and nonfunctional livers, we next examined repair responses to the accrued injuries. Accumulation of unfolded and misfolded proteins in the endoplasmic reticulum (ER) during ischemia activates the cellular stress mechanism referred to as the unfolded protein response (UPR) (13). Misfolded proteins bind to and activate protein kinase RNAactivated-like ER kinase (PERK) on the ER membrane, resulting in phosphorylation of eukaryotic initiation factor 2α (eIF2 α). The phosphorylation of eIF2 α leads to global inhibition of translation, initiation of antioxidant mechanisms, and induction of autophagy, the cell's repair and homeostasis mechanism (14). Analysis of eIF2 α by Western immunoblot demonstrated increased phosphorylation ratios of eIF2α in preperfusion biopsies in both groups [functional = 0.54] (IQR: 0.46-0.74) vs. nonfunctional = 0.69 (0.40-0.82), P =0.83 (Fig. 4A). After initiation of perfusion, both groups demonstrated a significant time-dependent decrease in phosphorylated eIF2 α (two-way ANOVA time factor P =0.0012), with negligible activation in functional livers after 6 h of perfusion [0.0084 (0.0067–0.030)], potentially indicating resolution of ER stress. Qualitatively, there was a trend toward higher levels of eIF2α phosphorylation in the nonfunctional livers [0.10 (0.010–0.13), P = 0.13], with liver N1 representing the outlier with the lowest ratio at 6 h. As noted

Figure 2. Comparison of differential gene expression patterns in functional and nonfunctional livers. A: three-dimensional (3-D) PCA plot demonstrates clustering of individual livers at 0, 3, and 6 h of perfusion (red: nonfunctional, green: functional). B: circular heatmaps for each group represent the top 10% of genes accounting for the variance in PC1. *FDR < 0.05 for either 3 h vs. 0 h or 6 h vs. 0 h comparison. C: volcano plots (FDR vs. fold change) comparing gene expression between time points in functional and nonfunctional livers. Genes meeting the FDR cutoff < 0.05 are shown in red (upregulated) and blue (downregulated); nonsignificant genes are shown in black. D: activation Z-scores of the top significant ($P < 10^{-14}$) upstream regulators from IPA enriched in both functional and nonfunctional groups at 3 and 6 h relative to preperfusion (0 h). E: heatmaps show differential expression of downstream gene targets for the top four upstream regulators (log₂FC shown for 3 h vs. 0 h and 6 h vs. 0 h comparisons, FDR cutoff <0.05); nonsignificant expression indicated by white space). F, functional livers; FDR, false discovery rate; IPA, ingenuity pathway analysis; N, nonfunctional livers; PC1, principal component 1; TNF, tumor necrosis factor; IL1 β , interleukin 1 β ; NF- κ B, nuclear factor- $\kappa\beta$ subunit; IFN γ , interferon γ .

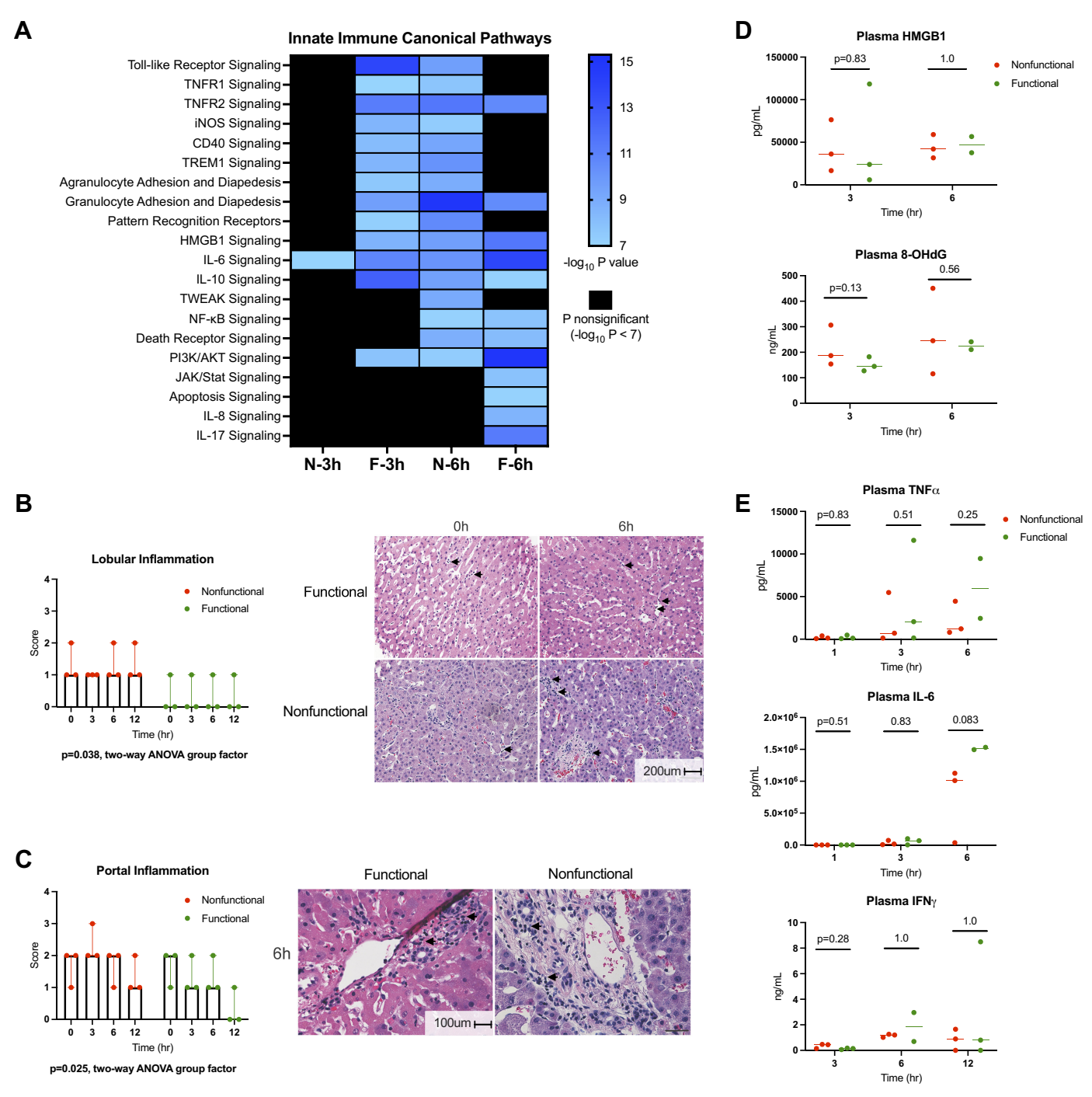
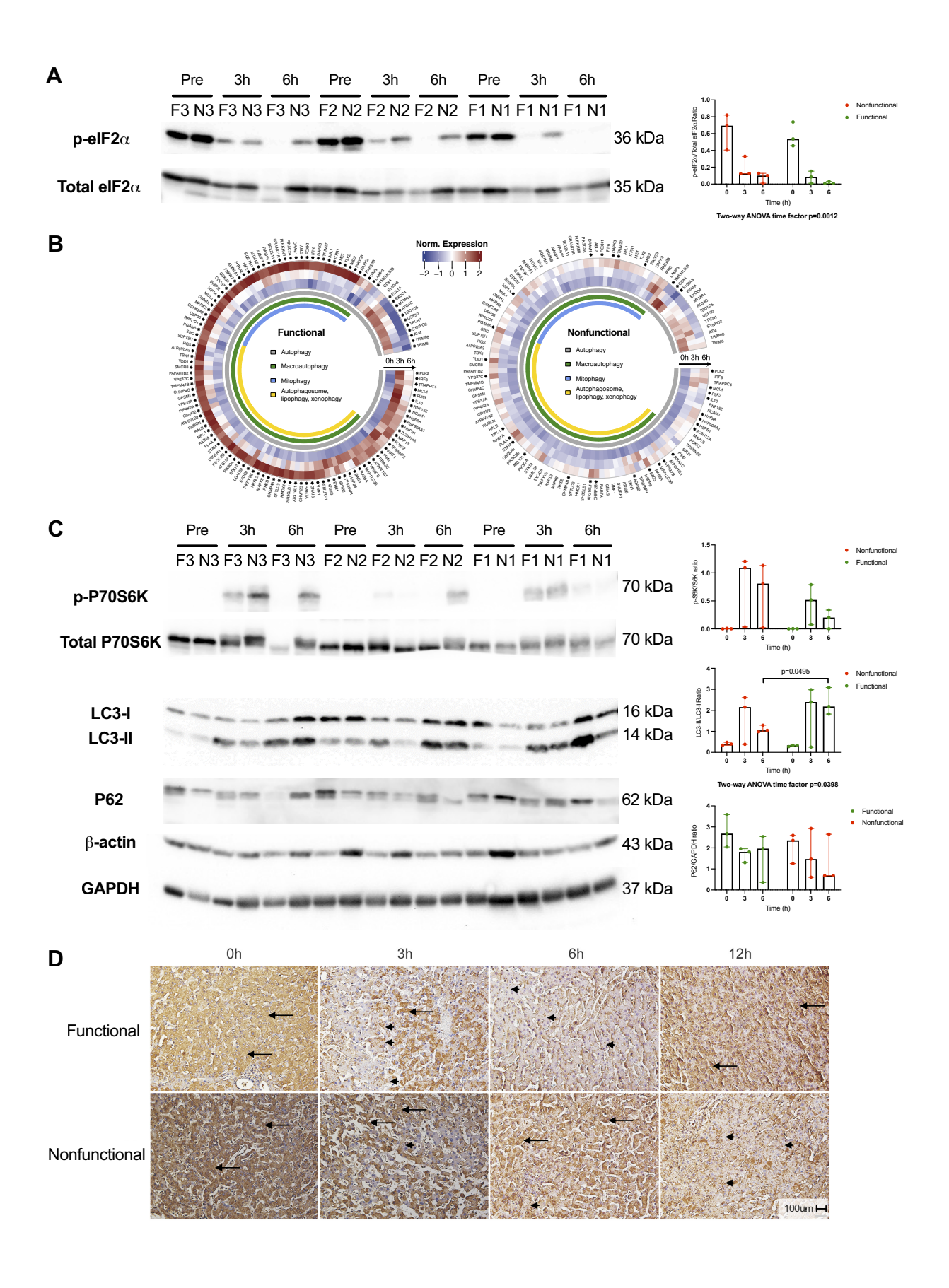


Figure 3. Ischemia-reperfusion injury and innate immunity in functional and nonfunctional livers. A: heatmap displays enrichment of canonical pathways related to innate immunity derived from IPA. The significance threshold was set to $-\log 10\ P$ value > 7 for comparisons of 3- and 6-h gene sets to preperfusion (0 h) baseline for each group. Lobular (B) and portal (C) inflammatory infiltrate as scored by a blinded pathologist. Representative H&E images for functional and nonfunctional livers are displayed. Scale bars: 200 μm (lobular), 100 μm (portal). D: damage-associated molecular pattern (HMGB1) and oxidative stress (8-OHdG) levels in circulating perfusate. Liver F2 6-h perfusate sample not available. E: perfusate levels of cytokines involved in IRI response. Liver F2 6-h perfusate sample not available. E: hematoxylin-eosin; HMGB1, high mobility group box 1; IFN γ , interferon γ ; IL-6, interleukin-6; IPA, ingenuity pathway analysis; JAK/STAT, Janus kinase/signal transducer and activator of transcription; N, nonfunctional livers (red); NF- κ B, nuclear factor- κ β subunit; 8-OHdG, 8-hydroxy-2′ deoxyguanosine; TNF α , tumor necrosis factor α .

previously, nonfunctional liver N1 was most transcriptionally similar to the functional group in PCA.

With respect to activation of autophagy, functional livers demonstrated a more robust response, with the majority of associated genes significantly increasing in expression after initiation of NMP compared with nonfunctional livers (Fig. 4B). The mechanistic Target of Rapamycin (mTOR) pathway plays a key role in regulating autophagy; active mTOR



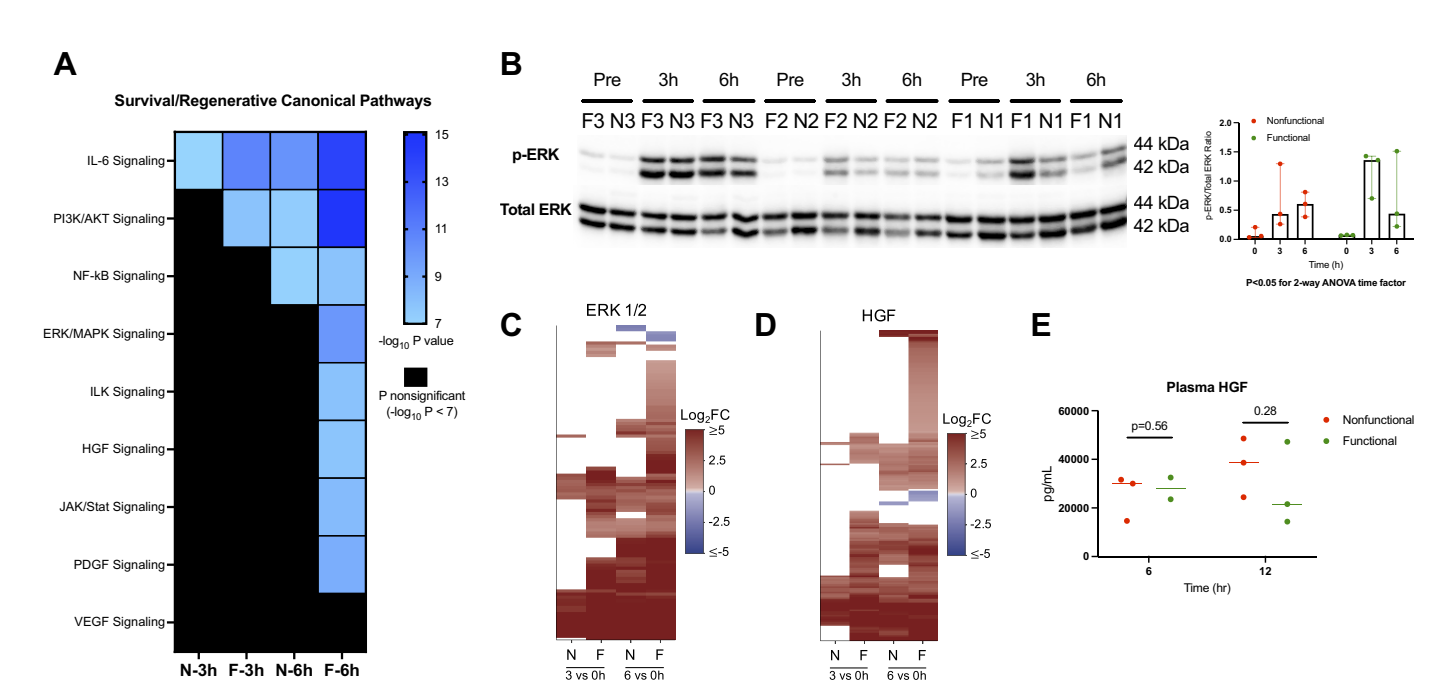


Figure 5. Prosurvival and regenerative signaling during NMP. A: heatmap displays enrichment of canonical pathways related to prosurvival and regenerative signaling derived from IPA. The significance threshold was set to $-\log 10\ P$ value > 7 for comparison of 3- and 6-h gene sets to the preperfusion (0 h) baseline for each group. B: Western blot of phosphorylated and total ERK (top) with densitometry ratios (bottom). C: heatmap displaying differential expression of downstream ERK targets in functional and nonfunctional livers ($\log_2 FC$ shown for 3 h vs. 0 h and 6 h vs. 0 h comparisons, FDR cutoff <0.05); nonsignificant expression indicated by white space). Target list derived from upstream regulator analysis in IPA. D: perfusate concentration of HGF in both groups after 6 and 12 h of NMP. Liver F2 6-h perfusate sample not available. E: heatmap of downstream gene target differential expression for HGF. F, functional livers; FDR, false discovery rate; HGF, hepatocyte growth factor; IPA, ingenuity pathway analysis; JAK/STAT, Janus kinase/signal transducer and activator of transcription; log2 FC, log2 fold change; N, nonfunctional livers; NF-κB, nuclear factor-κβ subunit; NMP, normothermic machine perfusion.

complex 1 inhibits autophagy through regulation of autophagy-related proteins and lysosome biogenesis (15). To assess mTOR complex 1 activation, we performed Western immunoblotting for phosphorylation of its downstream substrate p70 S6 kinase (p70S6K). Phospho-p70S6K was barely detectable before perfusion in both groups. In the functional livers, phosphorylation was increased at 3 h of perfusion and decreased by 6 h. In contrast, nonfunctional livers had high levels of phospho-p70S6K at both 3 and 6 h of perfusion (Fig. 4C). Comparisons between groups were nonsignificant due to an outlier, again nonfunctional liver N1. This liver had the lowest activated p70S6K protein ratio at 6 h (0.02) among the nonfunctional group despite having the highest ratio at 3 h (1.21), a pattern similar to the functional livers. In contrast, liver N2, the worst functioning nonfunctional liver, had a low ratio at 3 h (0.03) that greatly increased at 6 h (0.81). Despite not reaching statistical significance, the temporal pattern of p70S6K phosphorylation appeared consistent with sustained mTOR activation in nonfunctional livers.

Next, we investigated protein components involved in autophagic flux to determine if activation of autophagy was associated with liver function. The microtubule-associated

protein 1 light chain 3 (LC3) family is vital to autophagosome formation. Posttranslational modification of LC3 generates LC3-I, which is subsequently conjugated with phosphatidylethanolamine to generate LC3-II, the active protein necessary for elongation of the autophagosome membrane. Both functional and nonfunctional livers demonstrated a time-dependent increase in LC3-II:LC3-I ratio (two-way ANOVA time factor P = 0.0398), indicating autophagosome assembly in response to initiation of NMP (Fig. 4C). However, functional livers were found to have a significantly higher ratio after 6 h of NMP compared with nonfunctional livers [2.18 (1.82-3.09) vs. 1.05 (0.98-1.29), P = 0.0495], consistent with the counterregulatory action of p70S6K. Determination of P62 content by Western blot did not demonstrate protein buildup in either group. We further confirmed the LC3 results using immunohistochemistry. Preperfusion biopsies demonstrated hepatocyte LC3 staining in a pan-cytosolic pattern in both groups. In functional livers, LC3 staining changed to demonstrate a granule-type staining pattern at 3 and 6 h of NMP, indicating autophagosome formation in the functional livers. By 12 h of NMP, functional livers again

Figure 4. Activation of autophagy in response to injury and stress during NMP. A: Western blot of phosphorylated and total eIF2 α with densitometry ratios. B: circular heatmaps demonstrating differential expression of genes associated with the GO term "autophagy" in functional and nonfunctional livers. Asterisk (*) next to gene names indicates FDR < 0.05 for either 3 h vs. 0 h or 6 h vs. 0 h comparison. C: phospho-/total P70S6K, LC3-I/-II, and P62 Western blots for both groups with densitometry ratios. β-Actin and GAPDH levels are shown as control and demonstrate variability between human livers. D: representative images of LC3 immunohistochemistry shown for both groups. Scale bar: 100 μm. eIF2α, eukaryotic initiation factor 2α; FDR, false discovery rate; F, functional livers (green); GO, gene ontology; LC3-I/-II, light chain 3-I/II; F, nonfunctional livers (red); NMP, normothermic machine perfusion.

demonstrated pan-cytosolic LC3 staining. In contrast, nonfunctional livers displayed persistent pan-cytosolic and scant granule-type staining after 3 and 6 h, with more apparent granular staining by 12 h of NMP (Fig. 4D).

The final step in autophagy involves fusion of the autophagosome with lysosomes to form the autolysosome. Examination of the perfusate proteomic analysis results revealed that nonfunctional livers had significantly higher concentrations of the lysosomal components cathepsin D $[\log_2 \text{ fold change } (\log_2 FC) = -2.36 \text{ compared with func-}$ tional livers, FDR = 0.043], prosaposin ($log_2FC = -1.95$, FDR = 0.016), and hexosaminidase subunit- β (log₂FC = -3.02, FDR = 0.033) compared with functional livers at 3 h of NMP. A fourth protein, carboxypeptidase vitellogenic like, putatively involved in lysosomal function (16), was also enriched in nonfunctional liver perfusates (log₂FC = -4.12, FDR = 0.0014) (Supplemental Fig. S7). Confirmatory ELISA reinforced the proteomic analysis, demonstrating a fivefold greater abundance of cathepsin D in the perfusate of nonfunctional compared with functional livers [13,440 ng/mL (10,619–18,416) vs. 2,474 (1,514–2,946) at 3 h, P =0.0495; Supplemental Fig. S7]. Numerous additional lysosomal components, including other cathepsins, demonstrated a trend toward enrichment in the perfusate of nonfunctional livers ($log_2FC < -1$ compared with functional livers) but failed to meet the FDR cutoff (Supplemental Data Set S3).

Prosurvival Signaling Is More Active in Functional Livers

Finally, we investigated the relevance of prosurvival signaling in response to reperfusion injury during NMP. Our transcriptome analysis revealed abundant prosurvival and early regenerative signals in functional relative to nonfunctional livers. Of note, several prosurvival pathways were concurrently involved in innate immune signaling, highlighting the bridge between injury and recovery. In functional livers, pathway analysis showed enrichment of components of the IL-6 and phosphatidylinositol-4,5-bisphosphate 3-kinase/ AKT serine/threonine kinase (PI3K/AKT) canonical pathways by 3 h. Transcriptomic profiling and pathway analysis also showed activation by 6 h of downstream effectors: nuclear factor-κβ subunit (NF-κB), mitogen-activated protein kinase (ERK/MAPK), Janus kinase/signal transducer and activator of transcription (JAK/STAT), and hepatocyte growth factor (HGF) (Fig. 5A). In contrast, nonfunctional livers appeared to have limited enrichment of IL-6 signaling at 3 h and only subsequent activation of PI3K/AKT and NF-κB pathways by 6 h. To further examine the effects of prosurvival signaling, we assessed ERK1/2 activation by phospho-specific Western immunoblotting. There was a time-dependent increase in ERK activation in both groups after initiation of NMP (two-way ANOVA time factor P = 0.014), though without significant differences between groups (attributable to marked sample-to-sample variability; Fig. 5B). Interestingly, examination of gene expression downstream of ERK revealed fewer differentially expressed target genes in nonfunctional compared with functional livers, similar to the pattern seen in innate immune and autophagy signaling (Fig. 5C).

With respect to regenerative signaling, we again observed more robust downstream HGF target gene expression in

functional compared with nonfunctional livers (Fig. 5D). Despite this, no significant difference was seen between groups in the perfusate concentration of HGF after 6 or 12 h of NMP (Fig. 5E). The 12-h plasma sample was used in this case given that regenerative pathways are activated in delayed fashion. Similar to the pattern seen in innate immune responses, prosurvival and regenerative signaling in nonfunctional livers lagged behind those seen in functional livers. Consistently, gene expression in nonfunctional livers at 6 h resembled gene expression at 3 h in functional livers. Of note, we did not find any evidence of hepatocellular regeneration as indicated by significant expression of genes involved in cell cycle entry (Supplemental Fig. S8), although the 6-h perfusion timeframe may have been too early to detect these changes.

DISCUSSION

Limited knowledge of liver physiology as it relates to hepatocellular function during normothermic machine perfusion remains a barrier to optimizing the application of this strategy to improve donor liver utilization. In this study, we show discarded DCD human livers that demonstrate adequate hepatocellular function during NMP are characterized by an early innate immune response followed by activation of autophagy and prosurvival mechanisms. In contrast, livers with inadequate hepatocellular function are characterized by delayed gene induction, later onset of innate immune signaling, and diminished activation of autophagy and repair mechanisms in response to NMP. To our knowledge, this is the first study to profile the transcriptomic response of discarded human livers during NMP and highlight the potential relevance of injury and repair mechanisms in determining liver hepatocellular function.

One unanswered question forestalling widespread adoption of NMP is whether ex situ dynamic preservation facilitates rehabilitation of graft function or simply provides a platform to test liver viability. Our analysis of the transcriptome and plasma proteome of discarded DCD human livers demonstrates activation of innate immunity as the primary response to initiation of NMP, similar to ischemia-reperfusion injury (IRI) in clinical LT (17, 18). Graft hepatocellular function appeared to be associated with the ability to initiate cell repair and prosurvival mechanisms in response to the influx of proinflammatory effectors released after reperfusion, as well as the ability to mitigate subsequent injury. Despite similar perfusate concentrations of circulating cytokines and DAMPs, nonfunctional livers were characterized by delayed transcriptional activation of injury response pathways. As a result, proinflammatory signaling was initiated later in the perfusion time course and likely delayed activation of homeostatic mechanisms. In comparison, the innate immune response in functional livers was activated early on and transitioned to repair and survival signaling by 6 h. These data suggest that NMP facilitates repair mechanisms in response to IRI; however, its effectiveness may be dependent on perfusion duration and the severity of graft injury before initiation of NMP.

We examined the autophagy pathway using a multifaceted approach to determine if cellular repair and homeostasis mechanisms in response to reperfusion injury differed between functional and nonfunctional livers in the ex situ setting. Cold ischemia is known to induce ER stress through accumulation of unfolded and misfolded proteins, activating the unfolded protein response following reperfusion (13, 19). Our data indicate that ER stress resolves following initiation of NMP, as indicated by a time-dependent decrease in phosphorylated eIF2a. This effect was more pronounced in functional compared with nonfunctional livers. The consequences of persistent eIF2 α activation was seen in the expression of genes involved in protein synthesis. Inhibition of global protein synthesis is a principal function of phosphorylated eIF2α and less robust upregulation of genes involved in protein biosynthesis was seen in nonfunctional compared with functional livers (Fig. 2B). Moreover, the UPR restores ER homeostasis through activation of antioxidative mechanisms, amino acid transport, and autophagy, though sustained stress can activate prodeath signaling (14). We interpret our results as indicating that activation of the UPR by ER stress and the resulting balance between recovery and cell death is essential to determining hepatocellular function during NMP.

At the transcriptome level, functional livers demonstrated more changes in the expression of genes associated with autophagy than did nonfunctional livers. Active autophagy in functional livers was evidenced by higher LC3-II:LC3-I protein ratios after 6 h of perfusion. In contrast, persistent p70S6K activation in nonfunctional livers likely resulted in repression of autophagy during the critical juncture of the liver's response to injury and stress during NMP. These data support the importance of repair and homeostatic mechanisms in determining hepatocellular function. Additional evidence gleaned from proteomic analysis of the circulating perfusate showed significantly higher concentrations of several lysosomal acid hydrolases in nonfunctional livers. Lysosomal damage and membrane permeabilization from overwhelming cellular injury releases cathepsins and hydrolases, which activate a cascade of cell death pathways, including apoptosis, necroptosis, and pyroptosis (15). Hyperactivation of such injury and stress response mechanisms appears to be detrimental to liver function. By extension, the key to facilitating graft repair or rehabilitation may be the minimization of these responses. Prior work has demonstrated the therapeutic value of inhibiting cathepsins in mitigating hepatic IRI (20), reflecting the potential benefit of minimizing the propagation of hepatocellular injury (21, 22). Future pivotal investigations aimed at restoring autophagy while decreasing cell death may be of significant clinical relevance (23).

Another key element of graft hepatocellular function appears to be the ability to activate and propagate prosurvival signaling. Our data are consistent with a major role for IL-6 in the immediate response to reperfusion in both groups, but enrichment of noninjurious survival signaling was seen only in functional livers later in the perfusion time course. Upstream regulators involved in growth and survival also demonstrated more robust activation as early as 3 h in functional compared with nonfunctional livers. Examination of proteins involved in early cell cycle entry did not reveal any evidence of hepatocellular regeneration. However, we consider it likely that 6 h of perfusion detailed here is of too short a duration to induce the sort of rapid cell cycle entry that is seen in rodent and human partial hepatectomy models (24, 25).

Our study had several noteworthy limitations. The first was a small sample size that limited our ability to distinguish more nuanced differences between groups. Livers included in the study were chosen from a larger cohort of grafts that included additional differentiating factors, such as donation after brain death and steatosis (8). We chose to prioritize a homogeneous cohort for analysis at the cost of a smaller sample size, though we found notable variability between livers in each group. This was a limiting factor in our study and may have hindered identification of significant genes in the time-static comparisons, particularly since liver N2 demonstrated a more severe injury profile than N1 and N3. Despite this, we were able to find statistically and clinically significant differences in temporal RNA and protein level changes that have important implications for future studies on targeted therapeutics and potential biomarkers of liver function. The second limitation was that livers were not able to be transplanted, thus precluding our ability to validate the empirical criteria for determining hepatocellular function. Rather than create new criteria, we made use of benchmarks currently available. The study results will also aid in understanding whether the chosen criteria need to be adjusted before wider clinical validation. In addition, the absence of regulatory approval for any machine perfusion device outside the scope of a clinical trial at the time of this study in the United States prevented us from transplanting these discarded grafts. Notably, the prerequisite clinical trials required to demonstrate device safety and efficacy in standard-criteria donors are were in progress during this study. Finally, we did not closely examine cholangiocellular function due to technical (cannulation) issues with bile collection and as the requisite single-cell analysis or sequential bile duct biopsies necessary was beyond the scope of this study. It is increasingly accepted that NMP alone does not prevent biliary complications after LT. Therefore, additional interventions such as hypothermic-oxygenated perfusion may be required to minimize ischemic biliary injury to prevent posttransplant cholangiopathy, a particularly relevant issue for DCD livers (26).

In conclusion, our study offers a detailed examination of the injury and repair mechanisms induced during normothermic machine perfusion of discarded DCD human livers. Livers that demonstrated adequate hepatocellular function were characterized by more effective activation of autophagy and repair mechanisms in response to ischemia-reperfusion injury. Based on our results, therapeutic targeting of these pathways during NMP may improve hepatocellular function, thus allowing their use in transplantation.

DATA AVAILABILITY

The data sets generated and/or analyzed during the current study are available in the Gene Expression Omnibus with Accession No. GSE165568.

SUPPLEMENTAL DATA

Supplemental Data Sets S1, S2, and S3: https://doi.org/10.5061/ dryad.f7m0cfxx0.



Supplemental Methods and Figs. S1-S8: https://doi.org/ 10.5281/zenodo.5206547.

ACKNOWLEDGMENTS

We thank the donors, their families, New England Donor Services, and LiveOnNewYork for making this work possible.

GRANTS

A.O. and J.C.S. are supported by National Institute of Environmental Health Sciences (T32ES007272). S.R. and H.Y. are supported by the Massachusetts General Hospital Executive Committee on Research. This research was funded by the National Institutes of Diabetes and Digestive and Kidney Diseases (R01DK096075, R01DK107875, and R01DK114506), the National Science Foundation (EEC 1941543, ATP-Bio), and the Rhode Island Hospital/Brown University Department of Pediatrics. We thank the University of Arkansas Proteomics Core, which is supported by National Institutes of Health Grant Nos. R24GM137786, P20GM121293, and S100D026736, for their valuable input and for processing our samples.

DISCLOSURES

K.U. is an inventor on pending patents relevant to this study and has a provisional patent application relevant to this study. K.U. has a financial interest in Organ Solutions, a company focused on developing organ preservation technology. K.U.'s interests are managed by the Massachusetts General Hospital and Mass General Brigham in accordance with their conflict of interest policies. None of the other authors has any conflicts of interest, financial or otherwise, to disclose.

AUTHOR CONTRIBUTIONS

A.O., S.R., J.C.S., K.U., P.A.G., J.A.S., and H.Y. conceived and designed research; A.O., S.R., M.G.H., J.M.B., C.C., and S.G.B. performed experiments; A.O., S.R., J.C.S., M.G.H., J.M.B., N.P., C.C., S.G.B., J.A.S., and H.Y. analyzed data; A.O., S.R., J.C.S., M.G.H., J.M.B., N.P., K.U., P.A.G., J.A.S., and H.Y. interpreted results of experiments; A.O., S.R., J.C.S., M.G.H., and J.M.B. prepared figures; A.O., S.R., and J.C.S. drafted manuscript; A.O., S.R., K.U., P.A.G., J.A.S., and H.Y. edited and revised manuscript; A.O., S.R., J.C.S., M.G.H., J.M.B., N.P., C.C., S.G.B., K.U., P.A.G., J.A.S., and H.Y. approved final version of manuscript.

REFERENCES

- 1. Vodkin I, Kuo A. Extended criteria donors in liver transplantation. Clin Liver Dis 21: 289-301, 2017. doi:10.1016/j.cld.2016.12.004.
- US Department of Health and Human Services. Scientific Registry of Transplant Recipients (SRTR) Health Resources and Services Administration. https://www.srtr.org/reports-tools/opo-specificreports/ [2020 Jan 5].
- Mergental H, Laing RW, Kirkham AJ, Perera M, Boteon YL, Attard J, Barton D, Curbishley S, Wilkhu M, Neil DAH, Hübscher SG, Muiesan P, Isaac JR, Roberts KJ, Abradelo M, Schlegel A, Ferguson J, Cilliers H, Bion J, Adams DH, Morris C, Friend PJ, Yap C, Afford SC, Mirza DF. Transplantation of discarded livers following viability testing with normothermic machine perfusion. Nat Commun 11: 2939, 2020. doi:10.1038/s41467-020-16251-3.
- Nasralla D, Coussios CC, Mergental H, Akhtar MZ, Butler AJ, Ceresa CDL, Chiocchia V, Dutton SJ, García-Valdecasas JC, Heaton N, Imber C, Jassem W, Jochmans I, Karani J, Knight SR, Kocabayoglu P, Malagò M, Mirza D, Morris PJ, Pallan A, Paul A, Pavel M, Perera MTPR, Pirenne J, Ravikumar R, Russell L, Upponi Watson CJE, Weissenbacher A, Ploeg RJ, Friend PJ; Consortium for Organ Preservation in Europe. A randomized trial

- of normothermic preservation in liver transplantation. Nature 557: 50-56, 2018. doi:10.1038/s41586-018-0047-9.
- Yeh H, Uygun K. Increasing donor liver utilization through machine perfusion. Hepatology 70: 431-433, 2019. doi:10.1002/ hep.30523.
- Jassem W, Xystrakis E, Ghnewa YG, Yuksel M, Pop O, Martinez-Llordella M, Jabri Y, Huang X, Lozano JJ, Quaglia A, Sanchez-Fueyo A, Coussios CC, Rela M, Friend P, Heaton N, Ma Y. Normothermic machine perfusion (NMP) inhibits proinflammatory responses in the liver and promotes regeneration. Hepatology 70: 682-695, 2019. doi:10.1002/hep.30475.
- Schlegel A, Dutkowski P. Letter to editor: repair or prevent: what is the real impact of normothermic machine perfusion in liver transplantation? Hepatology 70: 2231-2232, 2019. doi:10.1002/
- Raigani S, De Vries RJ, Carroll C, Chen YW, Chang DC, Shroff SG, Uygun K, Yeh H. Viability testing of discarded livers with normothermic machine perfusion: Alleviating the organ shortage outweighs the cost. Clin Transplant 34: e14069, 2020. doi:10.1111/ctr.14069.
- Karimian N, Matton AP, Westerkamp AC, Burlage LC, Op den Dries S, Leuvenink HG, Lisman T, Uygun K, Markmann JF, Porte RJ. Ex Situ normothermic machine perfusion of donor livers. J Vis Exp 19: e52688, 2015. doi:10.3791/52688
- van Leeuwen OB, de Vries Y, Fujiyoshi M, Nijsten MWN, Ubbink R, Pelgrim GJ, Werner MJM, Reyntjens K, van den Berg AP, de Boer MT, de Kleine RHJ, Lisman T, de Meijer VE, Porte RJ. Transplantation of high-risk donor livers after ex situ resuscitation and assessment using combined hypo- and normothermic machine perfusion: a prospective clinical trial. Ann Surg 270: 906-914, 2019. doi:10.1097/SLA.0000000000003540.
- Sanders JA, Lakhani A, Phornphutkul C, Wu KY, Gruppuso PA. The effect of rapamycin on DNA synthesis in multiple tissues from late gestation fetal and postnatal rats. Am J Physiol Cell Physiol 295: C406-C413, 2008. doi:10.1152/ajpcell.00450.2007.
- Gearing LJ, Cumming HE, Chapman R, Finkel AM, Woodhouse IB, Luu K, Gould JA, Forster SC, Hertzog PJ. CiiiDER: a tool for predicting and analysing transcription factor binding sites. PLoS One 14: e0215495, 2019. doi:10.1371/journal.pone.0215495.
- Emadali A. Nguyên DT. Rochon C. Tzimas GN. Metrakos PP. Chevet E. Distinct endoplasmic reticulum stress responses are triggered during human liver transplantation. J Pathol 207: 111-118, 2005. doi:10.1002/path.1798.
- Almanza A, Carlesso A, Chintha C, Creedican S, Doultsinos D, Leuzzi B, Luís A, McCarthy N, Montibeller L, More S, Papaioannou A, Püschel F, Sassano ML, Skoko J, Agostinis P, de Belleroche J, Eriksson LA, Fulda S, Gorman AM, Healy S, Kozlov A, Muñoz-Pinedo C, Rehm M, Chevet E, Samali A. Endoplasmic reticulum stress signalling - from basic mechanisms to clinical applications. FEBS J 286: 241-278, 2019. doi:10.1111/febs.14608.
- Zhu SY, Yao RQ, Li YX, Zhao PY, Ren C, Du XH, Yao YM. Lysosomal quality control of cell fate: a novel therapeutic target for human diseases. Cell Death Dis 11: 817, 2020. doi:10.1038/s41419-020-03032-5.
- Behrends C, Sowa ME, Gygi SP, Harper JW. Network organization of the human autophagy system. Nature 466: 68-76, 2010. doi:10.1038/nature09204.
- Zhai Y, Petrowsky H, Hong JC, Busuttil RW, Kupiec-Weglinski JW. Ischaemia-reperfusion injury in liver transplantation-from bench to bedside. Nat Rev Gastroenterol Hepatol 10: 79-89, 2013. doi:10.1038/nrgastro.2012.225.
- Sosa RA, Zarrinpar A, Rossetti M, Lassman CR, Naini BV, Datta N, Rao P, Harre N, Zheng Y, Spreafico R, Hoffmann A, Busuttil RW, Gjertson DW, Zhai Y, Kupiec-Weglinski JW, Reed EF. Early cytokine signatures of ischemia/reperfusion injury in human orthotopic liver transplantation. JCI Insight 1: e89679, 2016. doi:10.1172/jci.insight.89679.
- Liu X, Green RM. Endoplasmic reticulum stress and liver diseases. Liver Res 3: 55-64, 2019. doi:10.1016/j.livres.2019.01.002.
- Baskin-Bey ES, Canbay A, Bronk SF, Werneburg N, Guicciardi ME, Nyberg SL, Gores GJ. Cathepsin B inactivation attenuates hepatocyte apoptosis and liver damage in steatotic livers after cold ischemia-warm reperfusion injury. Am J Physiol Gastrointest Liver Physiol 288: G396-G402, 2005. doi:10.1152/ajpgi.00316.2004.

- Shen Y, Malik SA, Amir M, Kumar P, Cingolani F, Wen J, Liu Y, Zhao E, Farris AB, Raeman R, Czaja MJ. Decreased hepatocyte autophagy leads to synergistic IL-1 β and TNF mouse liver injury and inflammation. Hepatology 72: 595-608, 2020. doi:10.1002/hep.31209.
- Boteon YL, Laing R, Mergental H, Reynolds GM, Mirza DF, Afford SC, Bhogal RH. Mechanisms of autophagy activation in endothelial cell and their targeting during normothermic machine liver perfusion. World J Gastroenterol 23: 8443–8451, 2017. doi:10.3748/wjg.v23.i48.8443.
- Xu D, Zhao H, Jin M, Zhu H, Shan B, Geng J, Dziedzic SA, Amin P, Mifflin L, Naito MG, Najafov A, Xing J, Yan L, Liu J, Qin Y, Hu X, Wang H, Zhang M, Manuel VJ, Tan L, He Z, Sun ZJ, Lee VMY, Wagner G, Yuan J. Modulating TRADD to restore cellular homeostasis and inhibit apoptosis. Nature 587: 133-138, 2020. doi:10.1038/ s41586-020-2757-z.
- Michalopoulos GK, Bhushan B. Liver regeneration: biological and pathological mechanisms and implications. Nat Rev Gastroenterol Hepatol 18: 40-55, 2021. doi:10.1038/s41575-020-0342-4.
- Cho H, Lim IK, Lee J-H. Changes in the expression of cell cycle regulators during rat liver regeneration after partial hepatectomy. Exp Mol Med 28: 187-191, 1996. doi:10.1038/emm.1996.29.
- van Rijn R, Schurink IJ, de Vries Y, van den Berg AP, Cortes Cerisuelo M, Darwish Murad S, Erdmann JI, Gilbo N, de Haas RJ, Heaton N, van Hoek B, Huurman VAL, Jochmans I, van Leeuwen OB, de Meijer VE, Monbaliu D, Polak WG, Slangen JJG, Troisi RI, Vanlander A, de Jonge J, Porte RJ; DHOPE-DCD Trial Investigators. Hypothermic machine perfusion in liver transplantation - a randomized trial. N Engl J Med 384: 1391-1401, 2021. doi:10.1056/NEJMoa2031532.